INTERNATIONAL JOURNAL FOR NUMERICAL AND ANALYTICAL METHODS IN GEOMECHANICS, VOL. 21, 845–861 (1997)

STABILITY OF END-BEARING PILES IN A NON-HOMOGENEOUS ELASTIC FOUNDATION

R. P. WEST[1], M. E. HEELIS[1], M. N. PAVLOVIĆ[2]* AND G. B. WYLIE[3]

[1] *Department of Civil, Structural and Environmental Engineering, Trinity College, Dublin 2, Republic of Ireland*
[2] *Department of Civil Engineering, Imperial College, London, SW7 2BU, U.K.*
[3] *Cable and Wireless, London, WC1R 4QD, U.K.*

SUMMARY

The stability of end-bearing piles that are supported laterally along their entire length by an elastic Winkler foundation is investigated for the case when the coefficient of horizontal subgrade reaction varies linearly with depth. A pattern of clustering of buckling modes is shown to occur and the approximate modelling of the elastic foundation by averaging the stiffness of the subgrade is discussed. © 1997 by John Wiley & Sons, Ltd.

Int. J. Numer. Anal. Meth. Geomech., Vol. 21, 845–861 (1997)
(No. of Figures: 14 No. of Tables: 2 No. of Refs: 15)

Key words: buckling; end-bearing piles; Winkler elastic foundation

INTRODUCTION

Previous analytical treatments of the buckling of straight axially loaded piles completely embedded in elastic foundations have been based on the assumption that the foundations are homogeneous.[1,2] There are clearly many situations when this postulate is invalid.[3] However, it is generally accepted that the Winkler model does provide a reasonably accurate method for estimating the lateral response of piles.[4] The spring stiffness in the Winkler model (also known as the modulus of subgrade reaction) is widely used to estimate the lateral response of soils to pile movement. Its evaluation in the field varies with many parameters such as the breadth and stiffness of the pile and the intensity of the lateral load.[5] Guidance on its evaluation is presented elsewhere, for example West.[6] In their two papers, Eisenberger and Clastornik[7,8] solve the buckling problem allowing for heterogeneity in the foundation, but their method uses a finite element approach and, as will be shown, the buckling mode shapes can be complex even for linear variations in soil stiffness. Four elements can be required, even when the exact finite elements in the work of Eisenberger and Clastornik[7,8] are used, to produce accurate solutions for the buckling problem. The solution outlined in the present paper, on the other hand, is of the classical 'exact' type and, hence, lends itself readily to a parametric study of the problem under consideration.

This paper investigates the stability of an end-bearing pile restrained by an elastic foundation of linearly varying modulus of subgrade reaction along its length. An exact closed-form solution,

*Correspondence to M. N. Pavlović, Department of Civil Engineering, Imperial College, London, SW7 2BU, U.K.

CCC 0363–9061/97/120845–17$17.50

Received 15 October 1996
Revised 12 April 1997

similar to the one outlined in an earlier publication which investigated the related dynamic problem,[9] is derived. Any end conditions may be specified, but the results shown in this paper are for fixed–fixed, pinned–pinned and free–free end supports. (It should be clear that, whereas previous work has concentrated on the use of homogeneous foundations with symmetrical boundary conditions,[1] the method outlined in this paper enables any boundary conditions to be investigated for both homogeneous and non-homogeneous subgrade reaction.) The degree of end-fixity of real piles must naturally lie between a fixed and a free end condition. The buckling load of an end-bearing pile must, therefore, be bounded by the solutions presented here for fixed–fixed and free–free piles.

In this analysis the applied load remains vertical throughout and is resisted by end-bearing at the bottom of the pile. The more complex case of a follower applied load is considered elsewhere[10] using a discrete element approach.

It will be seen how it is possible to extend Hetényi's work on homogeneous foundations to show the existence of modal clusters, that is, sequential buckling modes that are almost identical in critical load. Clustering was also found to occur in the vibration problem of piles which are either partially or fully embedded in stiff foundations.[11] Due to the natural similarity of vibrational and buckling problems, therefore, it is anticipated that these model clusters will also emerge in the buckling case considered here. It has been shown in the vibration case that finite element analysis techniques cannot reliably predict the lowest mode when the modes are clustered[12] where, in certain circumstances, a higher mode is initially detected as the fundamental.[13] For this reason, and for convenience in parametric studies, a closed-form exact solution approach is adopted.

METHOD OF ANALYSIS

The governing equation for the deflected shape of a bar subjected to an axial compression force, P, and supported laterally by a Winkler foundation, is[1]

$$\mathrm{EI}\frac{\mathrm{d}^4 y}{\mathrm{d}x^4} + P\frac{\mathrm{d}^2 y}{\mathrm{d}x^2} + ky = 0 \tag{1}$$

where EI is the minimum flexural rigidity of the member and is constant along its length in the present analysis. The foundation stiffness parameter, k, is assumed to vary linearly with x, the distance below the top of the bar or pile, so that

$$k = k_0 + cx \tag{2}$$

where k_0 and c are constants for the foundation. k_l is defined as the maximum value of the stiffness parameter which exists at the bottom of the pile at $x = l$ (Figure 1). If the variable

$$\xi = \left(\frac{k_0 + cl}{\mathrm{EI}}\right)^{1/4}(x - l) = \alpha(x - l) \tag{3}$$

is introduced, then

$$x = \frac{\xi}{\alpha} + l \tag{4}$$

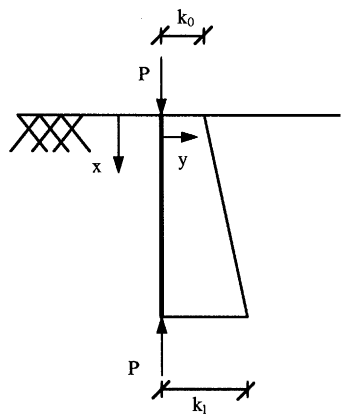

Figure 1. An axially loaded beam fully embedded in a linearly varying elastic foundation

It follows that

$$\mathrm{d}y/\mathrm{d}x = \alpha(\mathrm{d}y/\mathrm{d}\xi) \tag{5}$$

and, generally,

$$\mathrm{d}^n y/\mathrm{d}x^n = \alpha^n \,\mathrm{d}^n y/\mathrm{d}\xi^n \tag{6}$$

The governing equation with respect to ξ can now be formed as,

$$\frac{\mathrm{d}^4 y}{\mathrm{d}\xi^4} + \frac{P}{\alpha^2 \mathrm{EI}}\frac{\mathrm{d}^2 y}{\mathrm{d}\xi^2} + \frac{k_0 + \dfrac{c\xi}{\alpha} + cl}{\alpha^4 \mathrm{EI}} y = 0 \tag{7}$$

Now, let

$$\frac{P}{\alpha^2 \mathrm{EI}} = \frac{P}{\sqrt{(k_l \mathrm{EI})}} = \beta \tag{8}$$

Also, let

$$\frac{k_0 + \dfrac{c\xi}{\alpha} + cl}{\alpha^4 \mathrm{EI}} = \frac{k_l}{\alpha^4 \mathrm{EI}} + \frac{c\xi}{\alpha^5 \mathrm{EI}} = 1 + \gamma\xi \tag{9}$$

where

$$\gamma = c/(\alpha k_l) \tag{10}$$

Then, the dimensionless governing equation is

$$\frac{\mathrm{d}^4 y}{\mathrm{d}\xi^4} + \beta\frac{\mathrm{d}^2 y}{\mathrm{d}\xi^2} + (1 + \gamma\xi) y = 0 \tag{11}$$

Assuming a solution of the form

$$y = \sum_{n=0}^{\infty} a_n \xi^n \tag{12}$$

and substituting it into the dimensionless governing equation, the following recurrence relationship between the coefficients, a_n, is produced,

$$a_n = -\frac{\beta(n-2)!\,a_{n-2}}{n!} - \frac{(n-4)!\,a_{n-4}}{n!} - \frac{\gamma(n-4)!\,a_{n-5}}{n!} \tag{13}$$

By cancelling the factorials the following can be obtained:

$$a_n = -\frac{\beta a_{n-2}}{n(n-1)} - \frac{a_{n-4}}{n(n-1)(n-2)(n-3)} - \frac{\gamma a_{n-5}}{n(n-1)(n-2)(n-3)} \tag{14}$$

Since a_n is a linear function of a_0, a_1, a_2 and a_3, the general solution to the differential equation is

$$y = \sum_{i=0}^{3} A_i Y_i \tag{15}$$

where

$$Y_i = \xi^i + \sum_{n=4}^{\infty} a_n \xi^n \tag{16}$$

and for $n \leqslant 3$, $a_n = 1$ if $n = i$ or $a_n = 0$ if $n \neq i$. A_0–A_3 represent the four constants of integration.

To obtain the buckling load of the pile and the corresponding mode shape, the boundary conditions at the ends of the member must be specified. In the case of no rotational restriction, an expression for the bending moment must be obtained. In the case of no restraint of displacement in the y direction, an expression for the shear force is required. With respect to x, the conditions for zero displacement, slope, bending moment and shear force are, respectively,

$$y = 0, \qquad \frac{dy}{dx} = 0, \qquad \frac{d^2y}{dx^2} = 0 \quad \text{and} \quad \frac{d^3y}{dx^3} + \frac{P}{EI}\frac{dy}{dx} = 0 \tag{17–20}$$

but, with respect to ξ, this becomes

$$y = 0, \qquad \frac{dy}{d\xi} = 0, \qquad \frac{d^2y}{d\xi^2} = 0 \quad \text{and} \quad \frac{d^3y}{d\xi^3} + \beta\frac{dy}{d\xi} = 0 \tag{21–24}$$

The specification of the boundary conditions at the two ends of the pile yields four homogeneous equations which may be written as

$$[M]\mathbf{A} = 0 \tag{25}$$

where

$$\mathbf{A} = \begin{bmatrix} A_0 \\ A_1 \\ A_2 \\ A_3 \end{bmatrix} \tag{26}$$

and $[M]$ is formed using the following half matrices to define the boundary conditions, with one half matrix being evaluated at $x = 0$ and one at $x = l$;

$$[M_{\text{fixed}}] = \begin{bmatrix} Y_0(x) & Y_1(x) & Y_2(x) & Y_3(x) \\ Y'_0(x) & Y'_1(x) & Y'_2(x) & Y'_3(x) \end{bmatrix} \tag{27}$$

$$[M_{\text{pinned}}] = \begin{bmatrix} Y_0(x) & Y_1(x) & Y_2(x) & Y_3(x) \\ Y''_0(x) & Y''_1(x) & Y''_2(x) & Y''_3(x) \end{bmatrix} \tag{28}$$

$$[M_{\text{free}}] = \begin{bmatrix} Y''_0(x) & Y''_1(x) & Y''_2(x) & Y''_3(x) \\ Y'''_0(x) + \beta Y'_0(x) & Y'''_1(x) + \beta Y'_1(x) & Y'''_2(x) + \beta Y'_2(x) & Y'''_3(x) + \beta Y'_3(x) \end{bmatrix} \tag{29}$$

The condition $|M| = 0$ gives the eigenvalues corresponding to the buckling load of the pile. A modified sign count algorithm is used to find the eigenvalues which are expressed in terms of β.[6,14] Hence, the values of the constants of integration A_0–A_3 relative to each other are obtained for a particular eigenvalue and the buckling mode shape is calculated. The buckling force will be denoted here as P_{crit}.

It is now convenient to introduce the following non-dimensional parameters:

$$F = k_0/k_l, \qquad \lambda = \left(\frac{k_l l^4}{\text{EI}}\right)^{1/2} \quad \text{and} \quad \theta = P_{\text{crit}}/P_{\text{E}} \tag{30–32}$$

where P_{E} is the Euler buckling load of a simply supported beam with no elastic supports along its span and is given by $P_{\text{E}} = \pi^2 \text{EI}/l^2$. Parameters θ and λ are, respectively, the dimensionless buckling force and stiffness parameters as defined in Hetényi.[1] It would be expected that, as the stiffness of the supporting medium tends to zero, for the first mode of buckling of a simply supported structure θ tends to 1, while for a structure which is built-in at both supports θ tends to 4, as simple Euler theory predicts.

RESULTS

To limit the number of graphs produced in this paper, only the extreme case of $F = 0$ will be examined in detail, although the method used can be applied to any value of F. The two extreme cases of $F = 1$ and $F = 0$ are, clearly, relevant to actual soil conditions as they approximate idealized clay and sand conditions respectively.[3] There is also evidence that $F = 0$ can be used to model overconsolidated clays.[15]

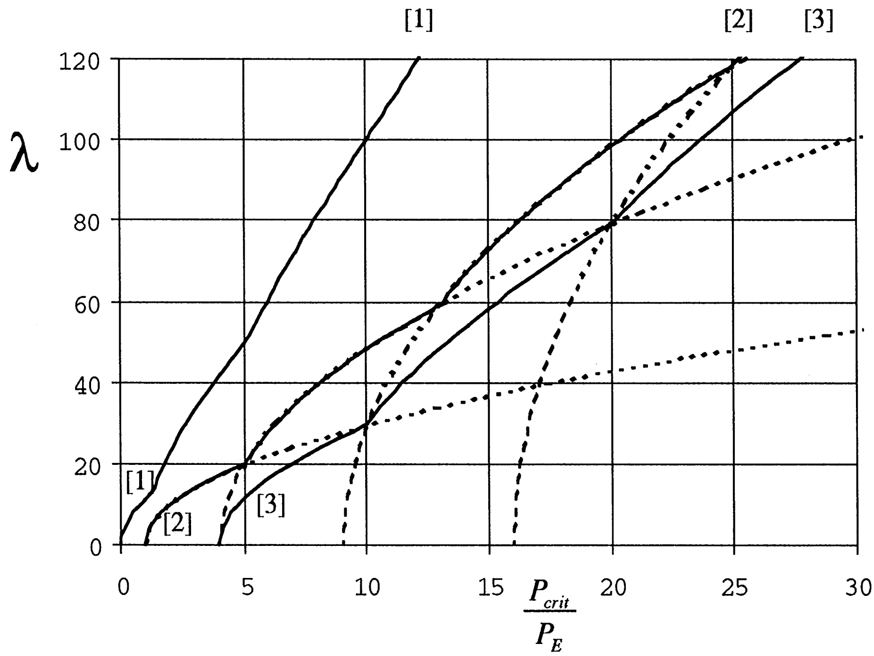

Figure 2. Buckling ratios for the first modes of a [1] free–free, [2] pinned–pinned and [3] fixed–fixed beam in a homogeneous soil (Hetényi [1946])

For the purposes of comparison, the exact $F = 0$ case will be compared with three further cases. The first two are the lower and upper bounds on θ for the two extreme cases of $k_0 = k_l = 0$ and uniform modulus $k_0 = k_l$ (that is, $F = 1$). Finally, it is interesting to investigate whether the actual system under study can be approximated by a simpler model in which the linearly varying stiffness is replaced by a uniform average stiffness along the length of the pile, that is, an approximate homogeneous foundation.

In Figure 2 the first buckling mode for the set of symmetric end conditions of a homogeneous foundation examined by Hetényi[1] have been plotted. As the soil stiffness parameter, λ, increases the plots can be divided into sections. In the case of the fixed–fixed beam, these sections can be easily seen as they occur between the intersections with the dotted mode cluster prediction lines at which point there is a discontinuity in the buckling load line. Similar discontinuities occur in the pinned–pinned case and the free–free case although in the free–free case they are not quite so easily distinguishable. Hetényi pointed out that each section has a particular mode shape associated with it, which can be characterized by the addition of a half wave as the soil stiffness increases. Note that all other graphs in this paper have the axes reversed from Hetényi, so that the dependent variable, the buckling load ratio, is on the vertical axis.

It is possible to predict the incidence of modal clusters and mode shape sections for symmetric boundary conditions with uniform soil stiffness (that is, $F = 1$) using formulae derived from Hetényi.[1] The modal clusters lie on the same lines that define the points where the first buckling

mode shape changed in the pinned–pinned and fixed–fixed case, Figure 2. These lines are parabolae defined by,

$$\frac{P_{\text{crit}}}{P_{\text{E}}} = n^2 + \frac{1}{\pi^4 n^2}\lambda^2 \tag{33}$$

where $n = 1, 2, 3, \ldots$ for the fixed–fixed, pinned–pinned and free–free cases. In the case of the free–free beam, however, the equation applies only to the buckling modes higher than the second. It should be noted that the mode clusters between modes also lie on straight lines which have equations of the form

$$P_{\text{crit}}/P_{\text{E}} = 4m^2 + 2\lambda/\pi^2 \tag{34}$$

where $m = 1, 2, 3, \ldots$ for fixed–fixed case and $m = 1/2, 1, 3/2, \ldots$ for pinned–pinned case. The first value of m indicates the line through the modal clusters between mode 1 and mode 2, the second value indicates the line through mode 3–mode 4 clusters, etc. For the free–free case, only modes higher than the second display these characteristic lines for values of $m = 1, 2, 3, \ldots$ The first and second mode clusters lie on a line which goes through the origin and has a gradient of half that in (34). Therefore, one can extend Hetényi's work to use the intersection of these parabolae and straight lines as a guide to where it would be expected that all modal clusters will occur. In Figure 3 these lines have been plotted for $F = 1$ in the fixed–fixed case. In this way, it is easier to understand what the extents of the different sections of the first modes are in Figure 2—they come from a wider trend in modal clustering.

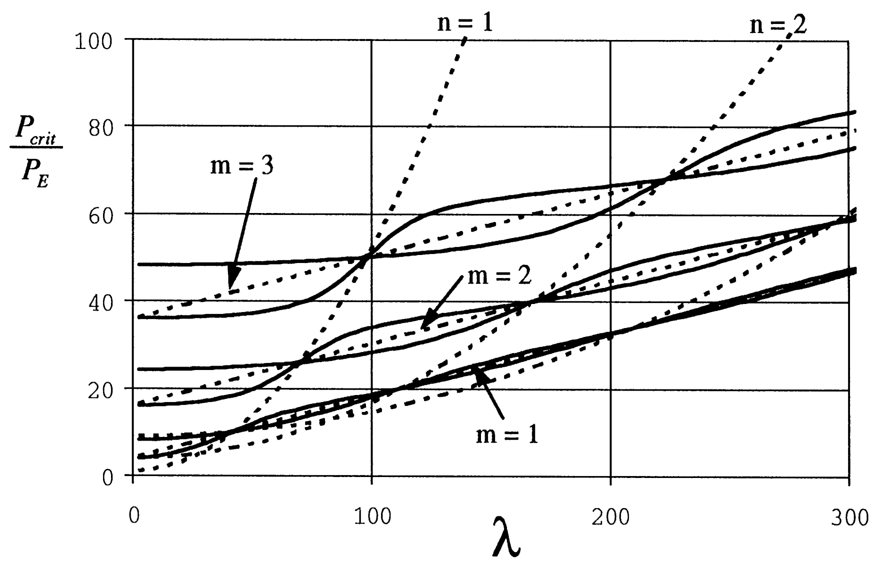

Figure 3. Buckling ratios for the first six modes of a fixed–fixed beam in a homogeneous soil ($F = 1$), ——, with the modal cluster prediction lines, - - - - (Hetényi [1946])

Table I. Buckling load of a fixed–fixed pile (EI $= 4\,\mathrm{MN\,m^2}$, length $= 3{\cdot}2$ m) in a homogeneous soil with $\lambda = 100$

Number of elements	Predicted buckling load (MN)
2	46·88
4	87·26
8	92·06
16	91·38
32	91·33
64	91·32
Exact solution	91·32

Table II. Buckling load of a pinned–pinned pile (EI $= 4\,\mathrm{MN\,m^2}$, length $= 3{\cdot}2$ m, 16 elements) in a homogeneous soil

λ	First mode detected (MN)	Second mode detected (MN)
19·7	19·215	19·262
19·8	19·301	19·372
19·9	19·528	19·340
20·0	19·380	19·686
20·1	19·419	19·845

In confirmation of the present approach consider Table I in which the finite element results for a fixed–fixed pile (with flexural rigidity of 4 MN m^2 and length 3·2 m) embedded in a homogeneous soil with soil stiffness parameter $\lambda = 100$ are presented. The buckling loads have been calculated using commercially available software based on the algorithm used by Lawther and Kabaila.[13] The results tend to the 'exact' result as the number of elements in the model was increased, as would be expected.

In Table II a problem with the use of some finite element packages is illustrated. When the soil stiffness approaches a modal cluster there is a tendency for the package to converge in a random fashion on either of the two clustering modes. In this way, for $\lambda = 19{\cdot}9$ the first mode converged on actually has a higher buckling load than the fundamental buckling mode (which is found second). The use of the closed-form solution and eigenvalue search algorithm presented here prevents this from occurring. This broadly concurs with the findings in the dynamics case.[12]

A parametric study of a fixed–fixed beam for the $F = 0$ case reveals a variation in θ for the first six buckling modes as shown in Figure 4. The sections indicated on the first, lowest mode are no longer as distinct as in Figure 2, although the individual sections have clear characteristic mode shapes (Figure 5). The changes in mode shape between the sections can be characterized by the addition of a half wave as previously. The mode shapes that occur during the transition from one section to another are of a complex nature.

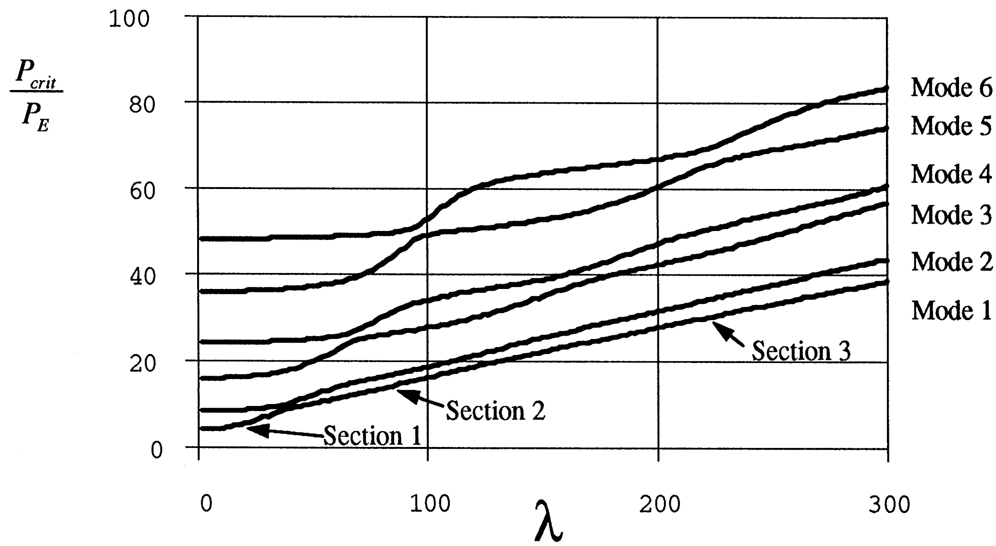

Figure 4. Buckling ratios for the first six modes of a fixed–fixed beam in a non-homogeneous soil ($F = 0$)

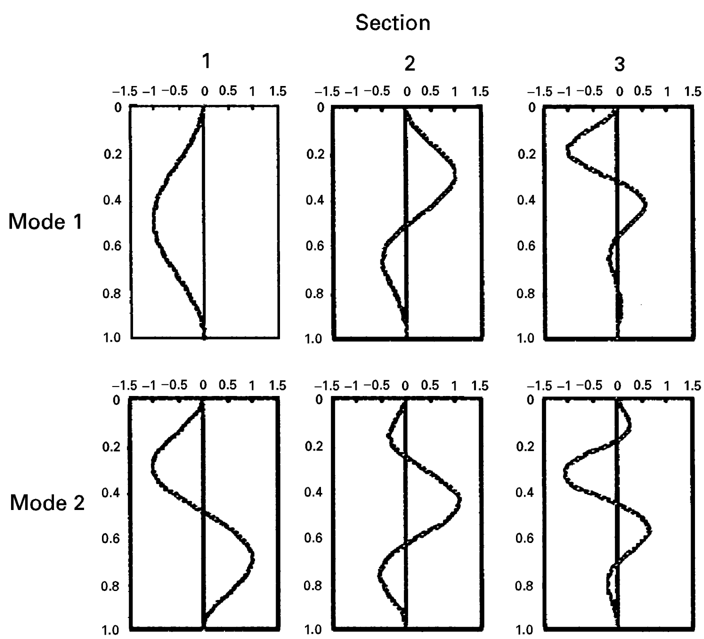

Figure 5. Mode shapes for modes 1 and 2 for the fixed–fixed case with $F = 0$

One is usually only interested in the lower modes and the lowest mode will normally be the first to be reached, but imperfections in the pile could mean that the second mode will be produced first. Also, attempts to strengthen a given pile by preventing particular modes developing have to be carefully considered. This could be of importance when in the proximity of modal cluster points. The inspection of higher modes is used here to investigate if there are any generic trends in their behaviour which will enable the prediction of trends in the lower modes, which are hard to recognize if only the lowest modes are considered. The closeness of modes also hinders finite element analysis of the problem:[12] thus in verifying results by the use of a finite element program using the method described by Lawther and Kabaila[13] it was found that, close to modal clusters, the analysis would converge on the second mode rather than the first mode, and this could lead to widely different mode shapes being predicted.

The lower-bound solution ($k_0 = k_l = 0$) is a set of constant values and, of course, it does not predict modal clustering. It should be noted that the solutions for θ in the $F = 0$ case approach the lower-bound solution as λ tends to 0 and this is a useful check on the method used. In this case (that is, $\lambda \approx 0$) the mode shapes predicted by the lower-bound solution are, of course, identical to those for the lowest section in the $F = 0$ case.

Equations (33) and (34) were derived by Hetényi (for $F = 1$) using a hyperbolic/trigonometric solution to the governing differential equations. In the $F = 1$ non-symmetric case the solutions can no longer be expressed simply in hyperbolic/trigonometric form. In the $F = 0$ symmetric end-fixity cases, the solutions to the buckling problem are of power series form and no simple expressions exist to predict where modal clusters occur. The question arises, will the use of an average soil stiffness predict modal clusters accurately?

If one approximates the $F = 0$ case with an average value of the two end stiffnesses and apply it uniformly over the length of the beam (that is, as if it were a homogeneous case) then the dimensionless buckling load associated with this approximation (denoted by θ_{est}) can be calculated by adjusting the value of stiffness λ for the $F = 1$ case. In this case of approximating for $F = 0$, the estimated (this is, averaged) stiffness, λ_{est}, relating to a particular mode shape and buckling force requires the stiffness λ to be divided by $\sqrt{2}$, that is

$$\lambda_{(F=1)} = \lambda_{\text{average}} = \left(\frac{1}{2}\frac{(0 + k_l)}{\text{EI}}\right)^{1/2} = \frac{1}{\sqrt{2}}\lambda_{(F=0)} \tag{35}$$

In Figure 6 the exact solution to $F = 0$ is plotted together with the average approximated result. For the higher modes using λ_{est} does enable both the buckling load and the relevant mode shapes to be estimated more accurately. A plot of mode shapes would show that they have the same number of half waves in both cases, it is just the relative amplitudes of these half waves that change.

Figure 7 shows where the modal cluster prediction lines occur for the $F = 0$ fixed–fixed case in relation to the exact solution in which the prediction lines have been plotted by using this average value of soil stiffness and substituting these values into equations (33) and (34). Note that mode clusters are accurately predicted for the higher modes. However, although mode 1 and mode 2 still have the changes between one mode shape and another predicted accurately by the estimated stiffness, there is no longer a straight line passing through successive clusters; in fact the approximation predicts clusters where there are none.

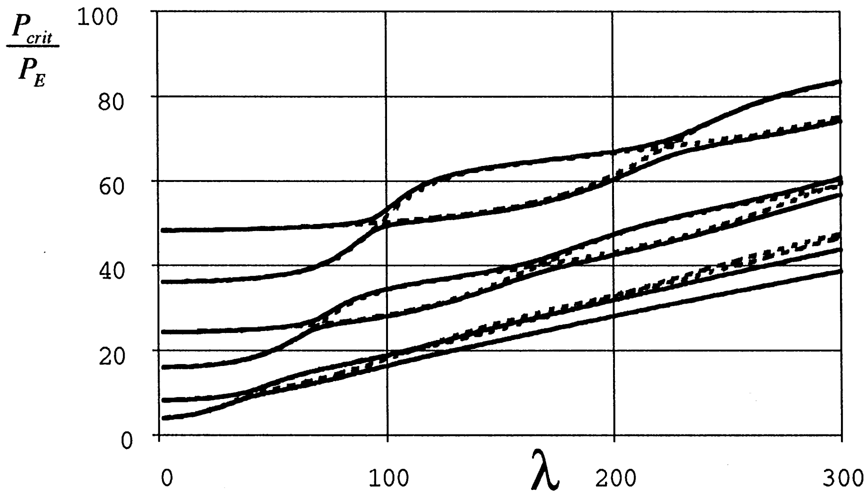

Figure 6. Comparison of $F = 0$, ——, and θ_{est}, - - - -, for the fixed–fixed case

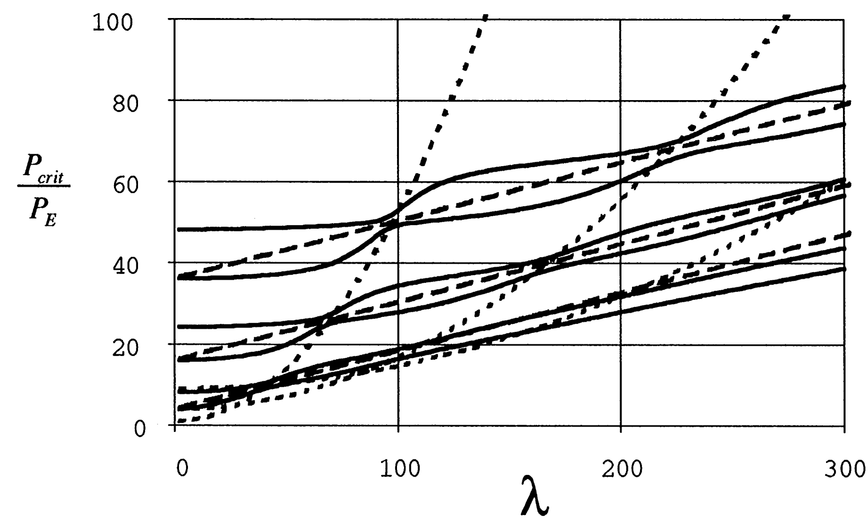

Figure 7. Predicting mode clusters using θ_{est}, - - - -, for the fixed–fixed case with $F = 0$, ——

Not surprisingly, the upper-bound solution ($k_0 = k_l$) in Figure 8 tends to overestimate the exact solution; for example, at $\lambda = 150$ the first mode is overestimated by about 50 per cent. The prediction of modal clusters is also inaccurate, as are the estimations of the corresponding modal shapes. The use of λ_{est} in Figure 6 means that the error at $\lambda = 150$ for the fixed–fixed case is reduced to about 3 percent. The error increases with soil stiffness, so that at $\lambda = 300$ the error is about 20 per cent.

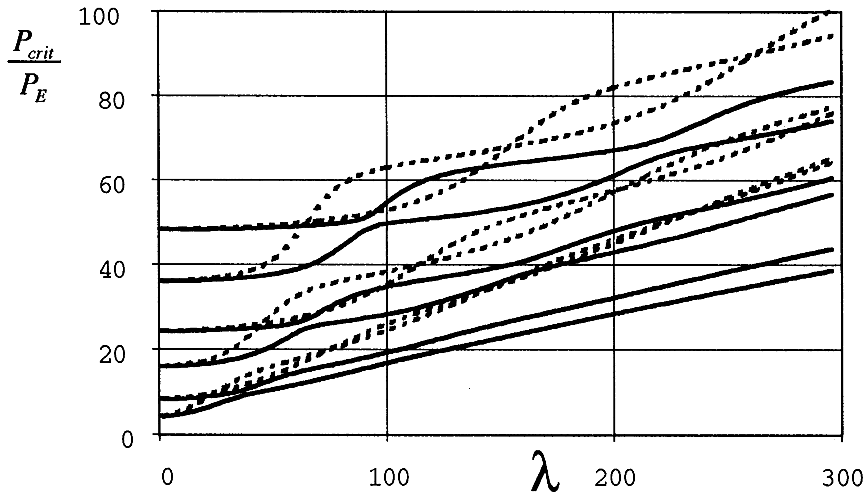

Figure 8. Comparison of $F = 0$, ——, and the upper-bound values for $F = 1$, - - - -, for the fixed–fixed case

The modal shapes corresponding to a linear soil stiffness compared to those given by an approximate constant one are noteworthy. In general, as soil stiffness increases there are frequent changes in modal shape from symmetric to anti-symmetric shapes as, of course, is the case with the homogeneous soil case.[1] In Figure 5 mode shapes have been plotted for the first two modes of the $F = 0$, fixed–fixed case. Sections 1 and 3 represent the mode shapes at $\lambda = 0$ and $\lambda = 300$ respectively. The middle shape represents the mode shape found after the first mode cluster in Figure 3, for example, when λ approximately equals 75. Figure 3 also indicates that, for the linearly increasing stiffness in a non-homogeneous soil, there are only three distinct mode shapes for the first mode since for $\lambda > 300$ there are no additional mode shape changes. An enlargement of Figure 3 would show how the three mode shapes are associated with the three sections (by sharpening the mode changeover—this is already clear for higher modes), but this is not obvious due to the scale of the diagram. This effect is caused by the larger stiffness at the bottom of the pile preventing displacements in all but the upper portion of the pile. For high soil stiffness, the pile produces approximately an Euler type buckling mode in the upper portion of the pile. This effect is equivalent to shortening the pile. A similar effect occurs for the second mode.

Considering the pinned–pinned case in Figure 9, it can be seen that the first mode for $F = 0$ is overestimated when an estimated uniform value of λ is used. At $\lambda = 150$ the overestimate is approximately 40 per cent while at $\lambda = 300$ it is approximately 60 per cent. This is because the buckling mode is concentrated at the upper end, where the soil stiffness is zero, the support of the soil at the bottom end of the pile being sufficient to restrain it in the vicinity. The effect also means that, as soil stiffness increases, the mode shape does not alter, and, hence, there are no mode clusters between the first and second modes. The use of an averaged λ can be seen to model higher modes quite well, yet, as discussed previously, it is the lower modes which are of interest. In the free–free case (Figure 10) it can be seen that θ_{est} overestimates the first mode by over 100 per cent at $\lambda = 300$. This is because, without the support at the upper portion of the pile, the member is able to buckle in this portion while not causing any deformation of the stiffer support at the

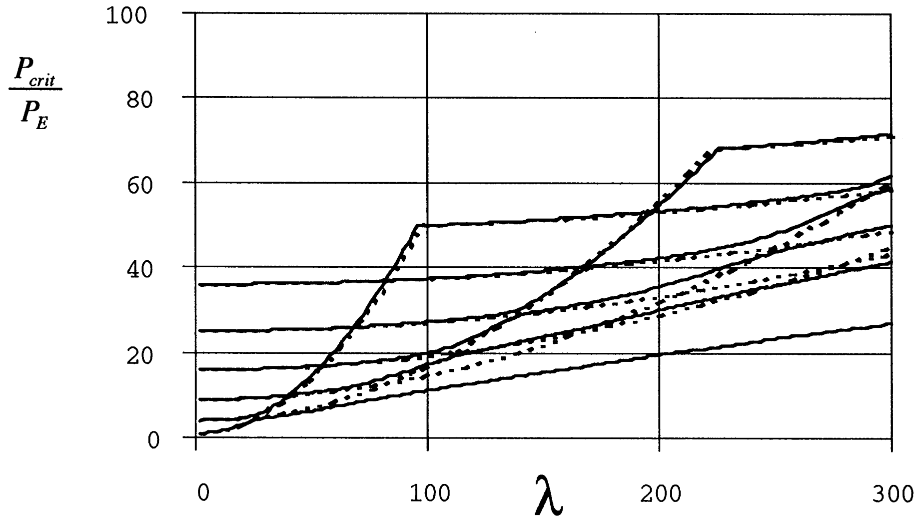

Figure 9. Comparison of $F = 0$, ——, and θ_{est}, - - - -, for the pinned–pinned case

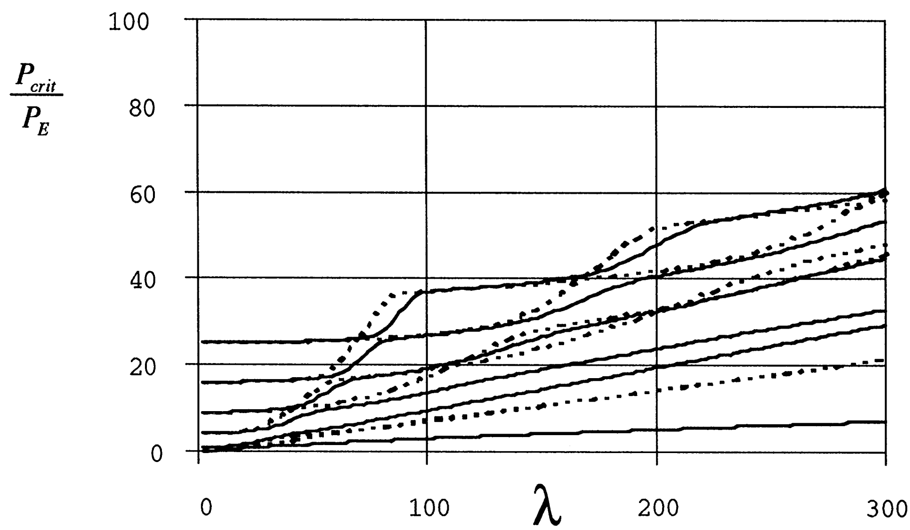

Figure 10. Comparison of $F = 0$, ——, and θ_{est}, - - - -, for the free–free case

bottom. It should also be noted that this means that, unlike the $F = 1$ case, the mode shapes are no longer symmetric or anti-symmetric (this being more pronounced now than in the fixed–fixed or pinned–pinned cases). As λ increases the mode shapes are quickly categorized as buckling in either the weakly or the well-supported sections, this support coming from the defined soil conditions. It can, thus, be deduced that the use of an average soil stiffness is particularly suspect when the end conditions are no longer fixed.

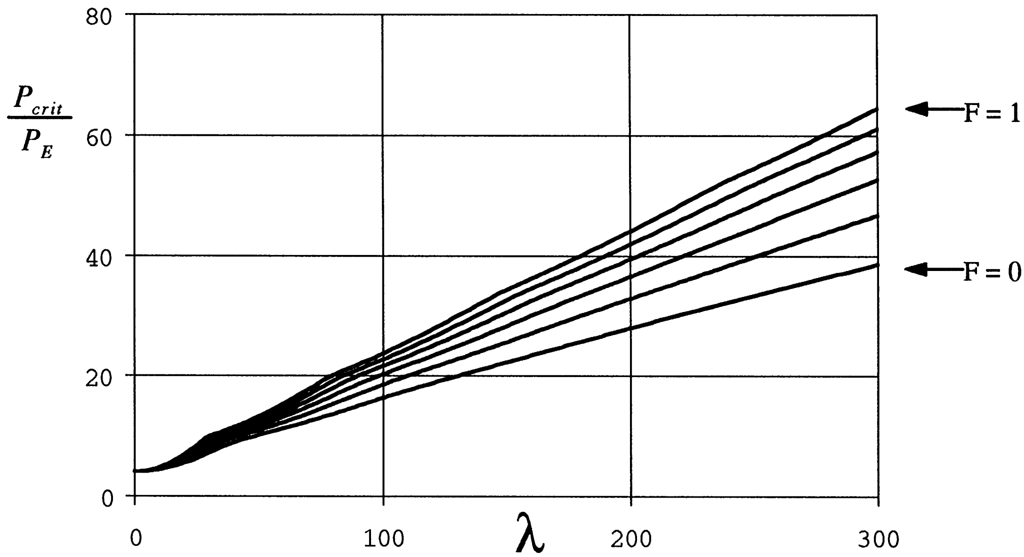

Figure 11. Mode 1 for $F = 0, 0{\cdot}2, 0{\cdot}4, 0{\cdot}6, 0{\cdot}8, 1$ for the fixed–fixed case

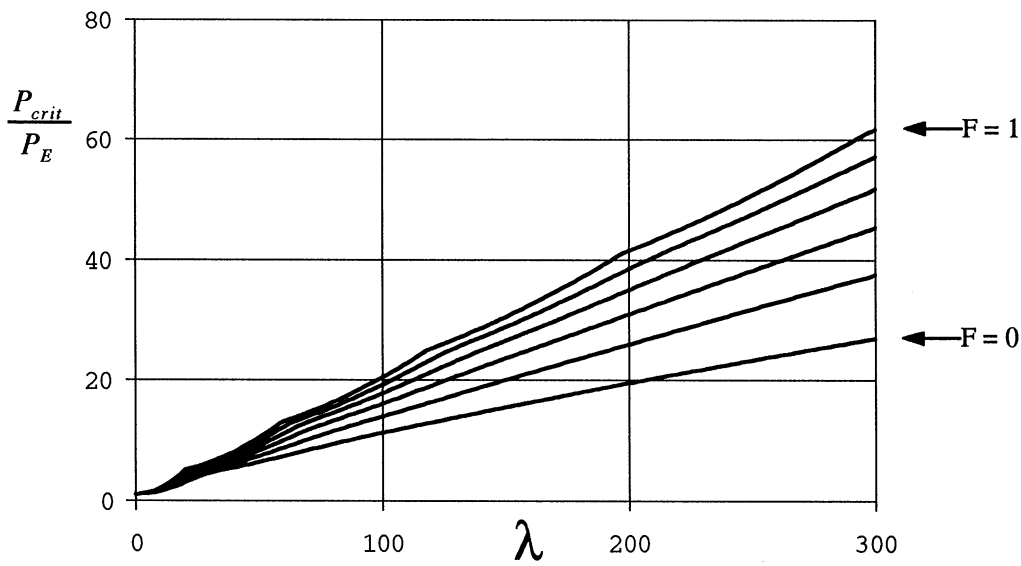

Figure 12. Mode 1 for $F = 0, 0{\cdot}2, 0{\cdot}4, 0{\cdot}6, 0{\cdot}8, 1$ for the pinned–pinned case

For completeness, Figures 11–13 illustrate the variation in the lowest buckling load as the soil conditions are varied between the two boundary cases of constant and linearly varying spring soil conditions for the fixed–fixed, pinned–pinned and free–free cases. The first buckling load is plotted in Figure 14 where all the possible combinations of end conditions are considered. Above

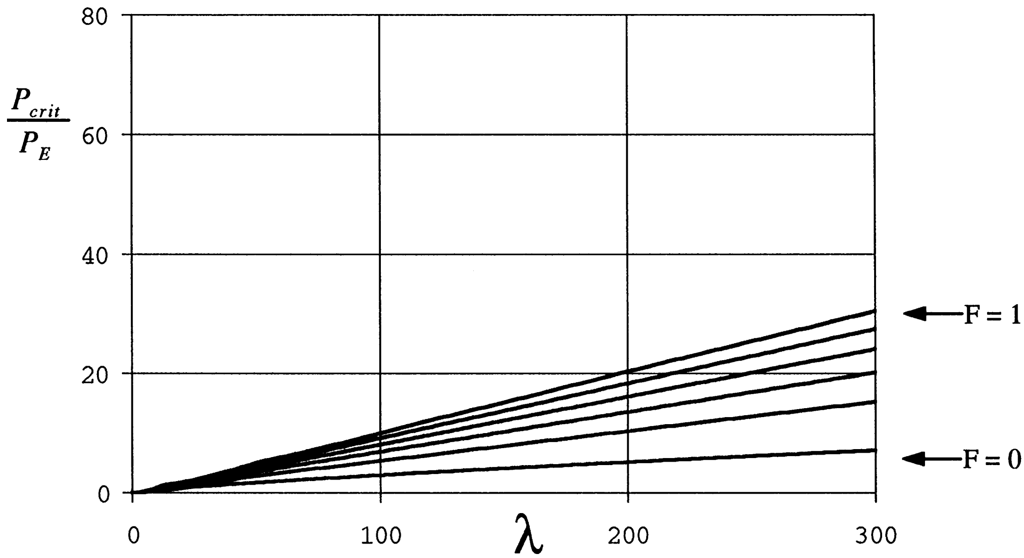

Figure 13. Mode 1 for $F = 0, 0{\cdot}2, 0{\cdot}4, 0{\cdot}6, 0{\cdot}8, 1$ for the free–free case

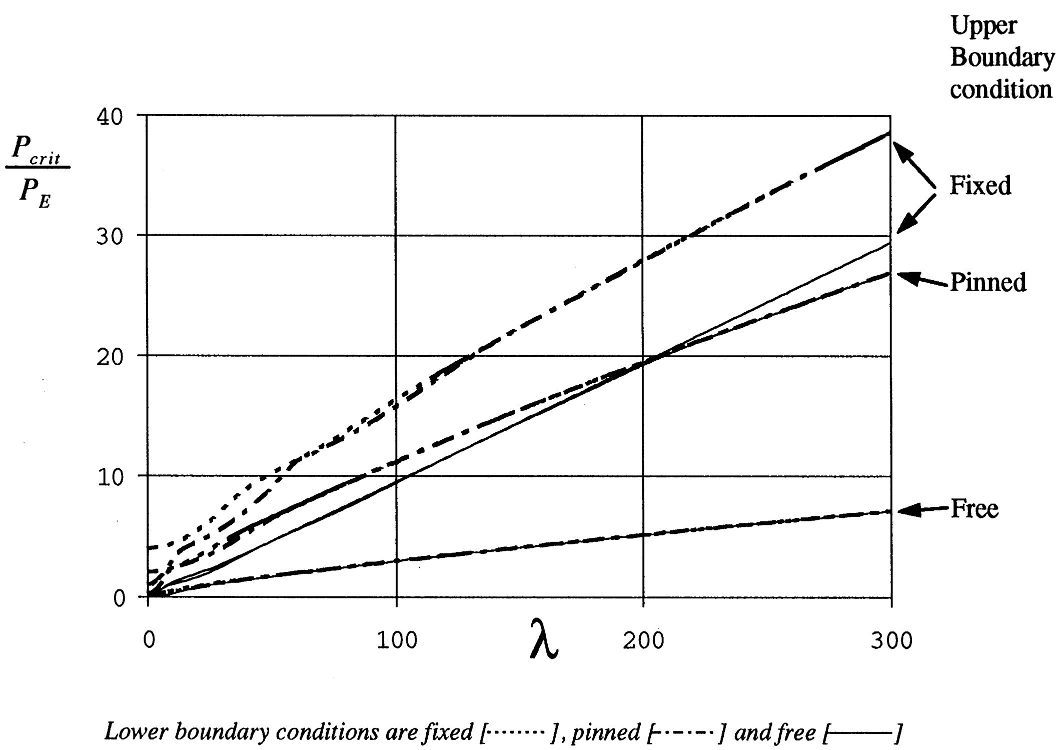

Figure 14. Mode 1 for $F = 0$ and all end conditions

$\lambda = 50$ the lower boundary condition does not affect the buckling load except when the upper boundary condition is fixed. Although not shown, the fixed–free fundamental buckling loads have been shown to coincide with the fixed–fixed results when $\lambda > 1100$.

CONCLUSIONS

An exact analytical solution has been presented in dimensionless form and a powerful computer algorithm has been developed to predict the buckling loads and mode shapes of a fully embedded Euler beam-column in an elastic Winkler foundation that increases its stiffness linearly with depth. Modal clustering has been recognized and a method of predicting when this occurs ahead of formal computations has been given by extending the work on homogeneous foundations carried out by Hetényi.[1]

Methods of approximating pile behaviour with simpler models have been discussed. These approximations can predict some modal clusters but are not sufficiently accurate to predict all modal changes. A pile with one of its ends unrestrained presents particular problems in this respect. It is not, however, possible to accurately model pile buckling loads by simple approximations such as the use of effective lengths and, hence, the algebraically exact method adopted in this paper should be used. The use of the lower-bound solution merely gives a useful check for low soil stiffness values. The method of averaging the soil stiffness along the whole pile can predict buckling loads more accurately in certain circumstances, although the method is not accurate enough for the lowest buckling modes.

It should be remembered that the first and, occasionally, the second modes are the most important. However, the analysis of higher modes can be used to recognize patterns in pile buckling behaviour and, hence, it is possible in this way to gain an understanding of the modal changes occurring in the lower, more critical, modes.

Classical end conditions (fixed and free) have been used in order to provide upper and lower bounds of the buckling load of an end-bearing pile. In reality, the fixity conditions at the top and bottom of a real pile must lie in between these two extremes and, therefore, limits on the solution are provided.

REFERENCES

1. M. Hetényi, *Beams on Elastic Foundation*, University of Michigan Press, Ann Arbor, 1946.
2. M. Eisenberger and D. Z. Yankelevsky, 'Exact stiffness matrix for beams on elastic foundation', *Comput. Struct.*, **21,** 1355–1359 (1985).
3. K. Terzaghi, 'Evaluation of coefficients of subgrade reaction', *Geotechnique*, **5,** 297–326 (1955).
4. L. C. Reese and R. C. Welch, 'Lateral loading of deep foundations in stiff clay', *J. Geotech. Div., ASCE*, **101,** 633–649 (1975).
5. CIRIA, 'Design of laterally loaded piles', *CIRIA Report* 103, London, 1984.
6. R. P. West, '*Modal clustering in the vibration of beams partially embedded in a Winkler foundation*', *Ph.D. Thesis*, Trinity College, Dublin, 1991.
7. M. Eisenberger and J. Clastornik, 'Beams on variable two-parameter elastic foundation', *J. Engng Mech. ASCE*, **113,** 1959–1966 (1987).
8. M. Eisenberger and J. Clastornik, 'Vibrations and buckling of a beam on a variable Winkler elastic foundation', *J. Sound Vib.*, **115,** 233–241 (1987).
9. M. N. Pavlović and G. B. Wylie, 'Vibration of beams on non-homogeneous elastic foundations' *Earthquake Engng Struct. Dyn.*, **11,** 797–808 (1983).
10. I. M. Smith, 'Discrete element analysis of pile instability', *Int. J. Numer. Anal. Meth. Geomech.*, **3,** 205–211 (1979).

11. M. N. Pavlović and R. P. West, 'Modal clustering in the vibration of partially and fully embedded steel piles', *J. Construct. Steel Res.*, **11,** 57–67 (1988).
12. R. P. West and M. N. Pavlović, 'Finite-element model sensitivity in the vibration of partially embedded beams', to be published.
13. R. Lawther and A. P. Kabaila, 'Modification of the power method for determination of eigenvalues', *Proc. 4th Int. Conf. on Finite Elements*, Australia, University of Melbourne, 1982.
14. R. P. West and M. N. Pavlović, 'A fast iterative algorithm for eigenvalue determination', in: B. H. V. Topping (ed.), *Developments in Computational Engineering Mechanics*, Civil-Comp Press 1993, pp. 229–236.
15. J. K. Atkinson, '*The deformation of undisturbed London clay*', *Ph.D. Thesis*, University of London, 1973.

